

WAVE GROUP FORCING OF LOW FREQUENCY SURF ZONE MOTION

MERRICK C. HALLER

707 Miller Ave. #2 Ann Arbor, MI 48103

Tel: (734) 663-8632

E-mail: merrick@coastal.Udel.edu

UDAY PUTREVU and JOAN OLTMAN-SHAY

NorthWest Research Associates, Inc., P.O. Box 3027, Bellevue, WA 98009

ROBERT A. DALRYMPLE

Center for Applied Coastal Research, Department of Civil Engineering,
University of Delaware, Newark, DE 19716

Received 18 November 1998

Revised 7 May 1999

The nearshore potential vorticity balance of Bowen and Holman (1989) is expanded to include the forcing from wave group-induced radiation stresses. Model results suggest that the forcing from these radiation stresses can drive oscillations in the longshore current that have a spatial structure similar to linear shear instabilities of the longshore current. In addition, the forced response is nearly resonant when the forcing has scales (k, σ) similar to the linearly most unstable mode. Thus, we suggest that wave groups may provide an initial perturbation necessary for the generation of shear instabilities of longshore currents and also act as a source of vortical motions on beaches where linear instabilities are completely damped.

Data from the SUPERDUCK (1986) field experiment were analyzed for the presence of spatially coherent wave groups. The analysis confirms that wave groups with periods and longshore spatial structures comparable to the observed shear wave motions were sometimes present on this open coast. This indicates that wave groups with the required spatial and temporal structure to initiate the low frequency oscillations in the longshore current can exist.

Keywords: Wave groups, shear waves, vorticity, longshore current, instabilities.

1. Introduction

Surf zone shear waves are low-frequency (10^{-3} to 10^{-2} Hz) vortical motions closely linked to the mean longshore current (Oltman-Shay *et al.*, 1989). Bowen and Holman (1989) suggested that shear waves are generated due to a shear instability of the mean longshore current. Subsequent work (see Shrira *et al.* (1997) for a complete set of references) has shown that the shear instability model is capable of explaining many of the observed characteristics. However, the instability theory fails to predict

the following two features — both related to the effects of bottom friction. First, the instability theory predicts a low-frequency cutoff below which no shear waves are generated (Dodd, 1994). Second, instability theory predicts that shear waves should be completely damped by friction on planar beaches. Both of these predictions are at odds with observations at Duck, NC and Santa Barbara (Leadbetter), CA beaches (Dodd *et al.*, 1992).

Recently, Shrira *et al.* (1997) showed that both shortcomings of the instability theory could potentially be explained by an explosive instability mechanism. In particular, Shrira *et al.* showed that shear waves that would otherwise be damped out by friction could grow due to resonant triad interactions, provided that their initial amplitudes exceed a critical value. However, how such initial (small amplitude) shear waves are generated remains unexplained. In this paper, we show that the direct forcing from wave groups could easily provide the initial shear wave amplitudes required by the triad interaction model. This mechanism follows earlier work by Hamilton and Dalrymple (1994).

The outline of this paper is as follows. In Sec. 2 the theoretical formulation is discussed. An example calculation in Sec. 3 shows that direct forcing from wave groups leads to a large response at shear wave scales, even when frictional dissipation precludes the existence of linear shear instabilities, thereby providing the initial amplitudes required by the triad interaction model. In Sec. 4, we analyze data from the SUPERDUCK experiment and find that there is some direct evidence that forcing at scales required to set up these initial oscillations existed. Data from the experiment at Leadbetter Beach could not be used in the wave group analysis because the offshore wave array was too short to resolve wave group scales. The final section is devoted to a few concluding remarks.

2. Theoretical Formulation

The depth-integrated, short-wave-averaged equations of horizontal momentum read

$$\frac{\partial u}{\partial t} + u \frac{\partial u}{\partial x} + v \frac{\partial u}{\partial y} = -g \frac{\partial \eta}{\partial x} + \tau_x - \frac{\tau_{xz}^b}{\rho h} \quad (1)$$

$$\frac{\partial v}{\partial t} + u \frac{\partial v}{\partial x} + v \frac{\partial v}{\partial y} = -g \frac{\partial \eta}{\partial y} + \tau_y - \frac{\tau_{yz}^b}{\rho h} \quad (2)$$

where u and v are depth-averaged horizontal velocities in the cross-shore (x) and longshore (y) directions, respectively; η is the free surface displacement; g is the acceleration due to gravity; $\tau_{\alpha z}^b$, $\alpha = x, y$, are the bottom shear stresses; and h is the total depth (it includes wave-induced set-down and set-up). Finally, τ_x and τ_y represent the forcing due to the radiation stresses.

We consider the case of a long straight coast. We separate all quantities into steady and time varying parts and assume that steady terms are independent of the

longshore coordinate, e.g.

$$\eta(x, y, t) = \eta_0(x) + \eta_1(x, y, t) \quad (3)$$

where η_1 represents the small ($|\eta_1| \ll |\eta_0|$) modulation effect of the wave groups. All other quantities are defined in an analogous fashion. We assume that the steady current has only a longshore component. That is, we assume

$$u = u_1(x, y, t) \quad (4)$$

$$v = V(x) + v_1(x, y, t) \quad (5)$$

Following Dodd *et al.* (1992), we parameterize the bottom friction using a linear law. In particular, we assume that $\tau_{xz}^b = \rho\mu u$, and $\tau_{yz}^b = \rho\mu v$, where $\mu = \frac{2}{\pi}c_f U_o$ is the friction coefficient, and U_o is the amplitude of the orbital velocity of the incident short waves and is assumed constant.

These definitions for velocity and bottom shear stress are now substituted into Eqs. (1) and (2). The resulting equations are separated into steady and unsteady parts. We find that the steady problem reduces to the familiar cross-shore momentum balance determining wave set-up and set-down, and the longshore momentum balance governing the generation of the mean longshore current. The unsteady problem is of particular interest here since it governs the dynamics of the low frequency motion in the nearshore. The linearized unsteady problem is governed by the following equations:

$$\frac{\partial u_1}{\partial t} + V \frac{\partial u_1}{\partial y} = -g \frac{\partial \eta_1}{\partial x} + \tau_{x,1} - \frac{\mu u_1}{h} \quad (6)$$

$$\frac{\partial v_1}{\partial t} + u_1 \frac{\partial V}{\partial x} + V \frac{\partial v_1}{\partial y} = -g \frac{\partial \eta_1}{\partial y} + \tau_{y,1} - \frac{\mu v_1}{h} \quad (7)$$

Following Bowen and Holman (1989), we make the rigid lid assumption; Falques and Iranzo (1994) have demonstrated the validity of this assumption for the class of motions being considered here. Therefore, the continuity equation becomes:

$$\frac{\partial(u_1 h)}{\partial x} + \frac{\partial(v_1 h)}{\partial y} = 0 \quad (8)$$

The nondivergence of the continuity equation allows us to introduce a transport stream function, Ψ , such that $\Psi_y = -u_1 h$ and $\Psi_x = v_1 h$ (subscripts (x, y) denote partial differentiation). Substituting the definition of the stream function into (6) and (7) and cross differentiating to eliminate η_1 leads to the following equation for the stream function:

$$\begin{aligned} & \left(\frac{\partial}{\partial t} + V \frac{\partial}{\partial y} + \frac{\mu}{h} \right) \left(\frac{\Psi_x h_x}{h^2} - \frac{\Psi_{yy}}{h} - \frac{\Psi_{xx}}{h} \right) + \Psi_y \left(\frac{V_x}{h} \right)_x + \frac{\mu h_x \Psi_x}{h^3} \\ & = \frac{\partial \tau_{x,1}}{\partial y} - \frac{\partial \tau_{y,1}}{\partial x} \end{aligned} \quad (9)$$

where subscripts denote partial differentiation (except for the definition of $\tau_{\alpha,1}$, $\alpha = x, y$). For simplicity, we concentrate on periodic solutions. Hence, we assume that the stream function may be expressed as

$$\Psi = \Re e\{\psi(x) e^{i(ky-\sigma t)}\} \quad (10)$$

where $\sigma = 2\pi/T$ ($T =$ wave period) represents the wave frequency and $k = 2\pi/L$ ($L =$ longshore wavelength) is the wavenumber. The amplitude of the stream function, $\psi(x)$, is in general complex. In addition, the forcing due to radiation stresses will also be assumed proportional to $e^{i(ky-\sigma t)}$, and expressed as

$$\frac{\partial \tau_{x,1}}{\partial y} - \frac{\partial \tau_{y,1}}{\partial x} = \Re e\{F(x, k) e^{i(ky-\sigma t)}\} \quad (11)$$

Substituting (10) and (11) into (9) and factoring out the periodic y, t dependency leads to

$$\left(V - \frac{\sigma}{k} - \frac{i\mu}{kh}\right) \left(\psi_{xx} - \psi k^2 - \frac{\psi_x h_x}{h}\right) - \psi h \left(\frac{V_x}{h}\right)_x + \frac{i\mu}{kh} \left(\frac{h_x}{h}\right) \psi_x = \frac{ihF}{k} \quad (12)$$

Note that the homogenous (unforced, $F = 0$) version of (12) is an eigenvalue problem. Nontrivial solutions for ψ , in the unforced problem, exist only for certain values of the eigenvalues, σ . These frequencies represent the natural frequencies of the system and they are, in general, complex; consequently, eigenvalues with positive imaginary parts represent unstable modes.

In the inhomogeneous problem, we calculate the steady-state response to the forcing due to wave groups. Since the forcing frequency is always purely real, the possibility of exact resonance is somewhat limited for this system. However, if the frequency mismatch is small, for example if the system is forced at (or near) the frequency of a neutrally stable mode, there is still a potential for a large forced response.

3. An Example Calculation

In this section, we present an example calculation that illustrates the nature of the forced response. First, we need to specify the longshore current, the wavenumber and frequency of the forcing, and the friction factor. For this example, we choose model parameters similar to those measured at Santa Barbara's Leadbetter beach. We make this choice because Dodd *et al.* (1992) found that the shear instability theory predicts shear waves should be damped out by friction on this planar beach.

The longshore current profile used in our calculations was generated using the model of Longuet-Higgins (1970). The model current profile (along with the measured current values) is shown in Fig. 1. It is noted that our model current profile contains somewhat more shear than that used by Dodd *et al.* (1992), this results in our profile being slightly more unstable than theirs. This difference should be kept in mind when comparing specific values of the friction factor between the two

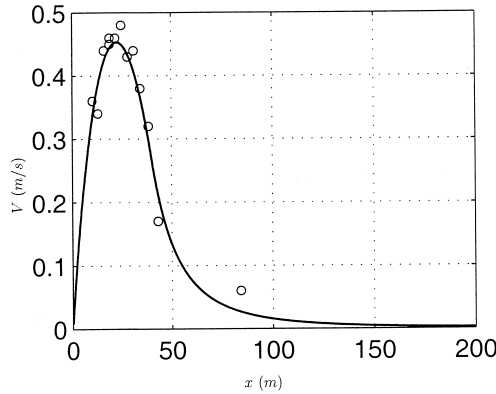


Fig. 1. Cross-shore variation of the modeled longshore current (solid line) using the model of Longuet-Higgins (1970), circles represent measured data from Leadbetter Beach, Santa Barbara, February 4, 1980. Note: $x = 0$ is the position of the mean shoreline.

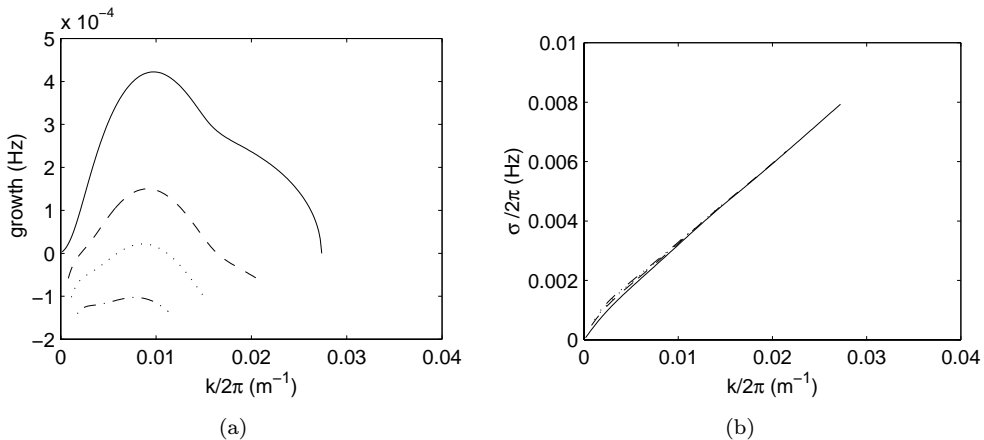


Fig. 2. (a) Linear growth rate ($Im[\sigma/2\pi]$) versus wavenumber and the (b) dispersion relation for the most unstable modes of the homogeneous system (12) ($F=0$) for the longshore current profile shown in Fig. 1 and friction coefficients: $\mu = 0$ (solid), 0.00269 m/s (dashed), 0.00399 m/s (dotted), and 0.00528 m/s (dash-dot).

studies; however, it is not critical to the nature of our results. To first get an estimate of the natural frequencies of the system, we solve the inviscid, homogeneous version of (12) (i.e. $\mu = 0, F = 0$). The results are shown as the solid lines in Fig. 2. Figure 2(a) shows the growth rates of the most unstable mode for each wavenumber and Fig. 2(b) shows the real part of the frequency.

Dodd *et al.* (1992) obtained a similar dispersion curve and stated that it compares reasonably well with observations, however, they also found that the inclusion of a realistic bottom friction will damp out the instability. Thus, the observations are unlikely to have resulted due to an instability of the longshore current profile. Here we investigate whether radiation stress forcing could have provided the small amplitude shear waves required of the triad interaction model.

In order to evaluate the forced response we must first specify the forcing function F . The work of Bowen (1969) suggests that the largest source of nearshore vorticity is the variation of radiation stresses within the surf zone. Similarly, Lippmann *et al.* (1997) find that the forcing of edge waves due to incident wave groups is largely confined to the surf zone. Therefore we will confine our forcing to the surf zone and assume that no forcing occurs seaward of the break point. In addition, following Foda and Mei (1981), we will assume a stationary break point as this allows for a simplified specification of the forcing. It is important to note that the exact form of the forcing function is not important for our purpose here, as long as the forcing function is not unreasonable.

Bowen (1969) derived the following radiation stress forcing term due to stationary wave height variations:

$$\frac{\partial \tau_{x,1}}{\partial y} - \frac{\partial \tau_{y,1}}{\partial x} = -\frac{1}{4} g \gamma \frac{\partial^2 H}{\partial x \partial y} \quad (13)$$

where γ is the ratio of wave height (H) to water depth in the surf zone and is assumed constant. Assuming, in our case, a planar beach and a longshore propagating wave height variation due to wave grouping [see Eq. (11)] we obtain the following forcing function:

$$F = -\frac{1}{4} i g \gamma^2 k h_x \epsilon \quad (14)$$

Here we consider the forcing due to the interaction of only two incident waves, and specify directly the forcing frequency (σ) and wavenumber (k) which results from the difference interaction of these incident waves. The modulation parameter ϵ represents the variation of the wave height about its mean value and here we choose $\epsilon = 0.05$ which is considered realistic for most field situations and is only half that assumed by Lippmann *et al.* (1997).

It should be noted that the forcing function (14) implies that the wave grouping persists to the shoreline, whereas in reality most wave grouping is transferred into a moving breaker point and is therefore destroyed in the breaking process. However, field data does suggest that wave grouping is not completely absent from the surf zone (List, 1991; Haller and Dalrymple, 1995). Therefore, we will further restrict the amplitude of the forcing term to exponentially decay ($\sim e^{-20(x/x_b-1)^2}$) from the breaker line (x_b) towards the shoreline. This limits (somewhat crudely) the forcing to a region very close to the zone of initial breaking. However, we will also show that our conclusions are not strongly influenced by this exponential decay.

As a measure of the forced response, we use the total kinetic energy averaged over a wavelength and period and integrated over x :

$$\overline{KE} = \int_0^\infty \frac{1}{TL} \int_0^T \int_0^L \frac{(u_1^2 + v_1^2)h}{2} dy dt dx \quad (15)$$

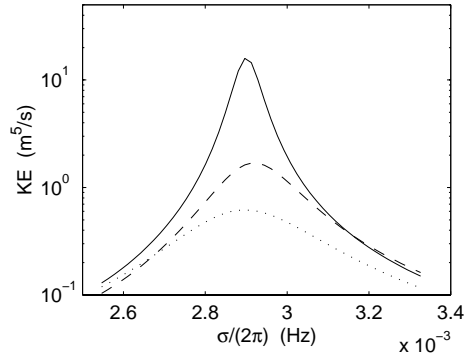


Fig. 3. The variation of kinetic energy **KE** as a function of the forcing frequency for a forcing spatial scale of $k/2\pi = 0.0097 \text{ m}^{-1}$. Shown are the forced system response [Eqs. (12) and (14) including exponential forcing decay] for three frictional coefficients: $\mu = 0.00269 \text{ m/s}$ (dashed), 0.00399 m/s (solid), and 0.00528 m/s (dotted).

The variation of shear wave kinetic energy, as a function of forcing frequency, is shown in Fig. 3 for a forcing spatial scale of $k/2\pi = 0.0097 \text{ m}^{-1}$ and for several friction coefficients, μ . This k value is chosen because it is the most unstable mode, i.e. it has the largest growth rate in the inviscid, homogeneous system [Fig. 2(a)].

The three values chosen for μ represent three different stability conditions. The value $\mu = 0.00269 \text{ m/s}$ is the value suggested by the model-data comparisons of Dodd *et al.* (1992). In their case, this value damped out any instabilities due to lesser shear in their velocity profile. In our case, this value of μ still allows free instabilities to grow, as can be seen in Fig. 2(a). In the second case, $\mu = 0.00399 \text{ m/s}$, the instability curve is nearly tangent to the neutral line as shown in Fig. 2(a). Interestingly, for the forced system, Fig. 3 shows that the largest response occurs when $\mu = 0.00399 \text{ m/s}$. This occurs because the natural frequency of the unforced system is almost completely real and therefore it most closely matches the real forcing frequency and the system is thus very close to resonance. The third case, $\mu = 0.00528 \text{ m/s}$, represents a condition when the free instabilities are damped out by bottom friction. This condition is most similar to what occurred at the Leadbetter Beach experiment. It is important to note that the μ value does not alter the frequency of the maximum kinetic energy (0.0029 Hz); the peak frequency consistently falls near the resonant frequency of the unforced system [0.0029 Hz in Fig. 2(b)], and the response shows an increased kinetic energy of an order of magnitude or larger near resonance for all μ values. These results indicate that if the system is forced at a broad range of frequencies it will preferentially excite its natural modes, even when these modes are damped by friction and would not exist in the unforced system.

Figure 4 shows the variation of the forced velocity amplitudes with offshore distance when the forcing scales (k, σ) nearly match the most unstable mode of the unforced system. The figure shows that the forced velocity amplitudes are largest

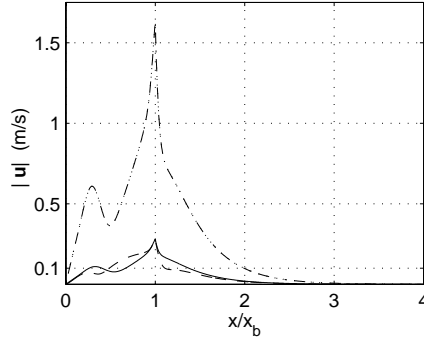


Fig. 4. Magnitude of calculated velocity amplitudes ($|\mathbf{u}| = \sqrt{u_1^2 + v_1^2}$) versus offshore distance for a forcing spatial scale of $k/2\pi = 0.0097 \text{ m}^{-1}$ and real frequency $\sigma/2\pi = 0.0029 \text{ Hz}$. Shown are the forced amplitudes for $\mu = 0.00528 \text{ m/s}$, with exponential forcing decay (solid), without decay (dashed), and $\mu = 0.00399 \text{ m/s}$ with forcing decay (dash-dot).

near the breaker line (x_b) and that the decay of the forcing function away from the breaker line does not strongly affect the response. Most importantly, this figure indicates that if the system is forced near its resonant unforced scales then the forced velocities can have significant magnitudes ($O(10 \text{ cm/s})$), even when the free instabilities are completely damped by friction. Shira *et al.* (1997) calculated that velocity perturbations exceeding a threshold of 4–11 cm/s would be necessary at Leadbetter beach in order to initiate resonant triad interactions leading to the generation of explosive instabilities. Figure 4 indicates that forced motions could exceed this threshold over a large part of the surf zone. In addition, the extremely large velocities for $\mu = 0.00399 \text{ m/s}$ point towards the potential for very large response when the instabilities are only nearly damped out. However, the influence of neglected terms would certainly restrain the response before such magnitudes were reached.

A comparison of the forced and free shear wave velocity fields is presented in Figs. 5 and 6. Figure 5 shows the velocity field of the free, undamped, shear instability ($\mu = 0, F = 0$). The pattern of this field is remarkably similar to the forced, damped shear wave field (Fig. 5, $\mu = 0.00399 \text{ m/s}$, F including exponential decay). Note that the longshore phase difference between the two figures is arbitrary.

Figures 3–6 suggest an alternative shear wave generation mechanism for a beach such as Leadbetter where shear waves cannot be generated from an instability of the longshore current (assuming realistic frictional damping and current profile). These figures show that given forcing with spatial and temporal scales near those of the shear waves, the system can preferentially excite frequency-wavenumber scales that satisfy the free system and generate wave patterns with similar form to the free, undamped shear waves. Given the magnitude of the forced motions, it is then plausible that they could resonantly grow via the explosive instability mechanism suggested by Shira *et al.* (1997).

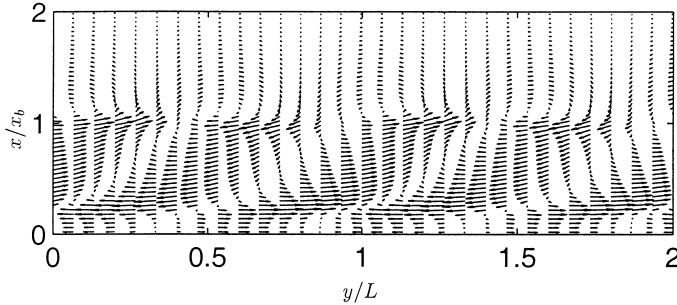


Fig. 5. Velocity distribution from solution of homogeneous system, $k/2\pi = 0.0097 \text{ m}^{-1}$. Absolute magnitude of these free instabilities is arbitrary.

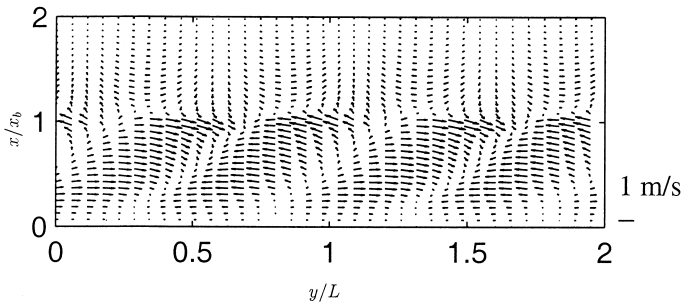


Fig. 6. Velocity distribution from solution of forced system including dissipation, $k/2\pi = 0.0097 \text{ m}^{-1}$, $\mu = 0.00399 \text{ m/s}$.

4. Field Data Analysis

The results from the calculations in Sec. 3 suggest that if wave group energy is present near the most unstable shear wave mode (from linear theory) in frequency-wavenumber space, the possibility of a near-resonant surf zone response to this forcing exists, and an explosive instability generation can occur. The work of Oltman-Shay *et al.* (1989) showed that shear waves reside in the lower end of the infragravity band ($0.001 < f < 0.01 \text{ Hz}$) with longshore wavelengths $100 < L < 1000 \text{ m}$. Typical two-dimensional (f, k) spectra of measured surf zone velocities (u, v) from the SUPERDUCK data set contain a ridge of energy spanning this range of frequencies and wavelengths.

Under most field conditions, the frequency spectrum of incident sea/swell waves is continuous and positive, i.e. there is some energy at all frequencies. The corresponding longshore wavenumber spectrum is also continuous and subject only to the following restriction:

$$|k_y| < (2\pi f)^2/g \quad (16)$$

where k_y is the longshore wavenumber of the incident waves and f is the frequency. Therefore, since wave groups occur at the difference frequencies and wavenumbers of

interacting pairs of sea/swell waves, wave group energy will span a wide range of frequencies and longshore wavenumbers with the strongest concentration at the lowest wave group frequencies but generally broad banded in longshore wavenumbers.

In the following section, we investigate certain field data to determine if the dominant (spatially coherent) modes of wave grouping at shear wave frequencies can be quantified and compared to shear wave length scales. Ideally, data from the Lead-better Beach experiment (Seymour, 1989) would be examined since the experimental conditions at that site most closely match those used in the modeling section of this paper. However, the offshore directional wave array during that field study was too short (6 m) to resolve wave group length scales. Instead, we used data from the SUPERDUCK experiment which had a much more extensive longshore directional wave array and therefore could be used to estimate dominant longshore wavelengths of wave groups at shear wave frequencies. We undertake this analysis, acknowledging that the wave group forcing mechanism is not required for the generation of shear waves on the barred coastline at the SUPERDUCK field site. Instead, our purpose is to quantify spatially coherent wave group scales at shear wave frequencies on an open coastal beach.

The SUPERDUCK experiment was hosted by the U.S. Army Corps of Engineers in October 1986 at Duck, North Carolina. The beach at this site trends NW-SE and is centrally located within a 100-km barrier spit (Crowson *et al.*, 1988). The beach slope is typically 1:20 in the surf zone and decreases to 1:200 offshore. In addition, the bathymetry is characterized by a three-dimensional bar system which often becomes linear during storms (Lippmann, 1989).

Surf zone velocity records were obtained from a longshore array of ten Marsh-McBirney bidirectional electromagnetic current meters located approximately 55 m offshore from the mean shoreline in the trough of the bar (Oltman-Shay *et al.*, 1989). The array had a minimum sensor separation of 10 m and total longshore extent of 510 m.

The incident wave climate was obtained by a linear array of 10 bottom-mounted pressure sensors located approximately 800 m offshore in 8 m water depth and spanning 255 m in the longshore direction. The array elements had a minimum sensor separation of 5 m. The wave fields measured during the experiment were highly variable but often consisted of longer period swell from the south along with shorter period wind-generated waves from the north and the surf zone usually extended approximately 100 m from the shoreline. Data for all sensors were sampled at 2 Hz during 4-hour measuring periods centered about high and low tides and the 4-hour tidal range was ~ 20 cm with a shoreline excursion of 2 m.

4.1. Offshore wave groupiness

To look for radiation stress forcing with similar scales to shear waves, we examine the incident wave envelopes associated with wave groups using the pressure records from

the offshore (8 m depth) array. Each of the pressure records were divided into sections 2048 s in length, demeaned and then detrended (using a least squares quadratic fit). The pressure records were converted to records of water surface elevation using the pressure response factor according to linear theory. The wave records were then bandpass filtered (0.06–0.30 Hz) to remove low (infragravity) frequency and high (wave harmonics, turbulence) frequency energy outside of the wind wave band. Time series of wave envelopes were computed from the filtered wave records using the Hilbert transform method (Melville, 1983). The specific data runs used in the present analysis represent a subset (6 runs of approximately 4 hours each) of the entire SUPERDUCK data set. Data selection was based on data quality and availability considerations. Almost all of the data runs that were available to us contained energetic shear wave motions, therefore little can be said about the presence of wave groups in the absence of shear waves during this experiment.

The incident wave conditions during the data runs used herein are considered typical for the field site. If a groupiness factor for each record is defined by $\sqrt{2} \cdot \sigma_A / \bar{A}$, where σ_A is the standard deviation of the wave envelope, \bar{A} is the mean, and GF varies from 0 to 1 (approximately), then the average GF for these records is ~ 0.75 ; suggesting significant wave grouping was present offshore of the surf zone during this experiment. It should be noted that GF is a somewhat limited measure which quantifies the sum of wave grouping over all wave group frequencies. This is separate from the modulation parameter ϵ used in Sec. 3 which represents the wave grouping at individual wave group frequencies. However, in the narrow banded limit the two measures would collapse to the same value.

4.2. Offshore wave groups and surf zone shear waves

Phase and coherence between the wave group time series of the offshore pressure sensors were calculated and plotted, as a function of sensor alongshore separation, to estimate the longshore scale and propagation direction of the incident wave groups. The offshore wave group phase and coherence plots were then compared with the (surf zone) shear wave phase and coherence plots computed from the longshore current records. All cross-spectra were computed using the standard Fast Fourier Transform method after first dividing each time series into 13 ensembles 2048 s in length with 50% overlap and tapering with a Hamming window. The number of spectral components was then reduced by half using a 2-point average resulting in a resolution of $\Delta f = 0.001$ Hz and 44 degrees of freedom (d.o.f.).

Using the longshore current records, the range of frequencies which contained spatially coherent shear waves was determined for each data run (usually 0.001–0.006 Hz, $\Delta f = 0.0009$ Hz). Typically, the shear waves demonstrated strong coherence for longshore distances of ~ 200 m. Oltman-Shay *et al.* (1989) showed that cross-shore current records also indicated coherent shear waves of similar scale. However, offshore wave group spatial coherence was found to typically be less than 100 m.

The tendency for wave groups to have low spatial coherence is not unexpected since wave grouping is likely a random process and is therefore broad banded in wavenumber at a given frequency. This is in contrast to shear waves, which are the result of a resonant process and tend to be narrow banded in wavenumber. In addition, wave group spectra tend to exhibit more statistical uncertainty than the original wave/current records and very long wave records are needed in order to obtain truly stationary estimates of wave grouping (Nelson *et al.*, 1988). To limit the processing of incoherent data, the offshore array was limited to six closely spaced sensors with a maximum lag of 90 m. The nearshore array was similarly limited to five sensors with a maximum lag of 130 m.

Using the wave group cross-spectra, the range of existing shear wave frequencies were searched for the presence of spatially coherent wave groups. Relatively, few cases were found in which the offshore wave groups were clearly shown to be dominated by scales similar to shear waves. In many cases, the wave groups did not exhibit significant coherence. In addition, there were cases where coherent wave groups existed but with scales different from shear waves and those will not be discussed here. It should again be stressed that wave groups are broad banded in frequency and wavenumber and that our search for dominant forcing scales is only to explore whether *spatially coherent* wave groups at the necessary scales exists at all.

The cases which best demonstrate that spatially coherent wave groups can exist offshore at similar spatial scales as shear waves are shown in Figs. 7–8. For comparison, the relative phase and coherence versus longshore lag of the shear waves is plotted together with those of the offshore wave groups. The slope (+/–) of phase versus lag indicates the direction of propagation (upcoast/downcoast) for the given motion and the figures show that the offshore wave groups at these frequencies were propagating in the same direction as the shear waves. The comparisons of coherence indicate that wave groups lose coherence at much shorter distances than shear waves (~ 50 m). The 85% confidence interval is also shown for reference (dashed

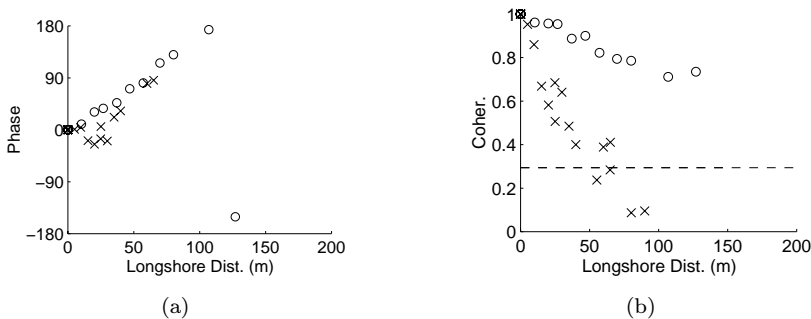


Fig. 7. Comparison of (a) relative phase versus lag, (b) coherence versus lag for shear waves (o) and offshore wave groups (x) at frequency 0.003 Hz. Dashed line represents 85% confidence interval, 44 d.o.f.. Data is from October 15 at 0945 EST sensors LA 1–6, LX 1–5.

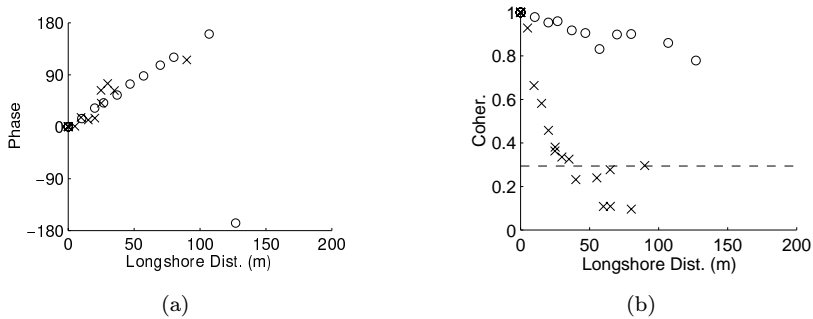


Fig. 8. Comparison of (a) relative phase versus lag, (b) coherence versus lag for shear waves (o) and offshore wave groups (x) at frequency 0.003 Hz. Dashed line represents 85% confidence interval, 44 d.o.f.. Data is from October 16 at 1020 EST sensors LA 1–6, LX 1–5.

line). The relative phase for lags which did not demonstrate coherence above the 85% confidence level are not plotted.

4.3. Surf zone wave groups and shear waves

The computations in Sec. 3 assumed that incident wave heights had a longshore progressive 2-D structure near the breaker line that swiftly decayed shoreward due to wave breaking. It is expected that any wave grouping present at the offshore array would persist and possibly increase in amplitude towards the breaker line due to shoaling. However, since the offshore array was about eight surf zone widths (x_b) from the shoreline, the cross-shore current records measured at the nearshore array (located $\sim x_b/2$) were also examined for any evidence of wave grouping persisting shoreward of the breaker line. To do this analysis, it must be assumed that, in the range of incident wave frequencies ($0.06 < f < 0.3$ Hz), the auto-spectra of the u velocities have the same shape as sea surface elevation spectra at the same location, since there were no pressure sensors in the nearshore array. The choice of cross-shore velocities for the wave group analysis was made because the u auto-spectra were more energetic at incident wave frequencies due to the near normal incidence of the waves at this nearshore location. The u velocity records were converted to surf zone wave (current) envelopes in the same manner as the offshore wave records (neglecting the pressure to water surface conversion).

A result from the phase and coherence analysis of the surf zone wave envelopes is shown in Fig. 9. The linear phase progression in the longshore direction allows an estimate of the dominant wave group length scale at this frequency during this data run and it appears similar to the shear wave scale. It should be noted that the bandpass filtering operation was tested with different windows (Hamming, Hanning) to rule out the possibility of leakage of the energetic shear wave motions into the incident wave band during filtering. The offshore wave envelopes did not show strong spatial coherence at this frequency suggesting that wave grouping was locally induced during this data run.

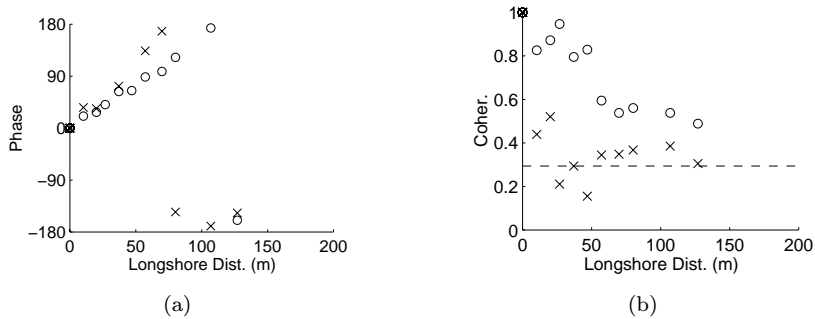


Fig. 9. Comparison of (a) relative phase versus lag, (b) coherence versus lag for shear waves (o) and surf zone wave groups determined from cross-shore velocity records (x) at frequency 0.003 Hz. Dashed line represents 85% confidence interval, 44 d.o.f.. Data is from October 18 at 1140 EST sensors LX 1–5.

The results of the cross-spectral analysis from SUPERDUCK data are presented here only to demonstrate that wave grouping at shear wave temporal and spatial scales can exist in the field. The calculations presented in Sec. 3 indicate that the response to such forcing will occur primarily at shear wave scales and that the velocity field will closely resemble the velocity field under free shear waves. Thus, it is suggested that direct forcing from wave groups could provide the initial perturbations required for shear wave growth. It is expected that on days when the longshore current is extremely weak and exhibits no inviscid instability characteristics, the presence of wave group forcing at shear wave scales would induce only a non-resonant forced response.

5. Conclusions

The inclusion of a forcing term due to wave group induced radiation stresses in the nearshore potential vorticity balance of Bowen and Holman (1989) shows that incident wave groups can force a surf zone response similar to shear waves. If the forced response has similar scales (k, σ) to the linear most unstable mode, the response is nearly resonant.

Natural beaches normally exhibit a wide range of wave group scales and it is expected that a certain amount of wave group energy will always be present at shear wave scales. However, we examined field data from a specific field site in order to examine whether wave groups with length and time scales corresponding to shear waves could occur. This was a difficult process, due to the broad banded wavenumber spread of wave groups at specific frequencies, and relatively few estimates of the dominant longshore wavelengths could be made. However, there were a limited number of cases where the dominant wave group length scale matched those of the observed shear waves at the same frequency, this field data demonstrates that wave grouping at shear wave scales was sometimes dominant during the SUPERDUCK experiment. The results indicate that wave grouping can exist

to perturb the nearshore velocity field at temporal and spatial scales of the shear instabilities.

In addition, it is interesting to view the results presented here in light of the recent work of Shira *et al.* (1997). Their work indicates that the range of unstable scales for shear waves excited by the explosive instability mechanism is much larger than that determined by the linear instability mechanism. This suggests that the presence of any of a wide range of coherent wave group spatial scales can force any of a wide range of initial instabilities to feed the explosive instability mechanism. Also, they show that the explosive instability occurs, even when all linear instabilities are damped by bottom friction, as long as the initial perturbations exceed a certain amplitude. Most importantly, the model described herein suggests that these initial perturbations can be provided by a relatively small amount of wave grouping.

The wave group forcing mechanism presented here and the results of Shira *et al.* (1997) provide a possible explanation for the observation of shear wave instabilities at Leadbetter Beach, CA. Dodd *et al.* (1992) found that linear instability theory did not predict instabilities for that beach unless the frictional damping was decreased by decreasing the frictional dissipation to unrealistic values. In light of the above, it can be hypothesized that the shear waves observed at Leadbetter Beach may have been generated via the explosive instability mechanism with wave groups providing the initial instabilities.

Acknowledgments

Funding for U. Putrevu and J. Oltman-Shay was provided by ONR Coastal Dynamics under contract number N00014-96-C-0075. Funding for M. Haller and R. Dalrymple was provided by the Army Research Office through University Research Initiative Grant DAAL 03-92-G-0116. The authors wish to thank Bob Hamilton for providing some of the software used in the data analysis and Bill Birkemeier, Peter Howd, Ed Thornton, and the staff at the Army Corps Field Research Facility (FRF) at Duck, NC, for their contributions to the field data acquisition and distribution (the 8 m array is still maintained as part of the FRF infrastructure).

References

- Bowen, A. J. (1969). Rip Currents, 1, Theoretical investigations, *J. Geophys. Res.* **74**: 5467–5478.
- Bowen, A. J. and R. A. Holman (1989). Shear instabilities of the mean longshore current, 1, Theory, *J. Geophys. Res.* **94**: 18023–18030.
- Crowson, R. A., W. A. Birkemeier, H. M. Klein and H. C. Miller (1988). SUPERDUCK nearshore processes experiment: Summary of studies, CERC Field Research Facility, Technical Report CERC-88-12, Coastal Eng. Res. Cent., Vicksburg, MS.
- Dodd, N., J. Oltman-Shay and E. B. Thornton (1992). Shear instabilities in the longshore current: A comparison of observation and theory, *J. Phys. Oceanogr.* **22**(1): pp. 62–82.
- Dodd, N. (1994). On the destabilization of a longshore current on a plane beach: Bottom shear stress, critical conditions, and onset of instability, *J. Geophys. Res.* **99**: 811–824.

- Falques, A. and V. Iranzo (1994). Numerical simulation of vorticity waves in the nearshore, *J. Geophys. Res.* **99**: 825–841.
- Foda, M. A. and C. C. Mei (1981). Nonlinear excitation of long-trapped waves by a group of short swells, *J. Fluid Mech.* **111**: 319–345.
- Haller, M. C. and R. A. Dalrymple (1995). Looking for wave groups in the surf zone, Proc. Coastal Dynamics '95, pp. 81–92.
- Hamilton, R. P. and R. A. Dalrymple (1994). Wave group forcing in low frequency surf zone motion, Center for Applied Coastal Research, Research Report CACR-94-23.
- Lippmann, T. (1989). The stability and spatial variability of sand bar morphology, MS Thesis, Oreg. State University, Corvallis.
- Lippmann, T., R. A. Holman and A. J. Bowen, (1997). Generation of edge waves in shallow water, *J. Geophys. Res.* **102**: 8663–8679.
- List, J. H. (1991). Wave groupiness variations in the nearshore, *Coastal Eng.* **15**: 475–496.
- Longuet-Higgins, M. S. (1970). Longshore currents generated by obliquely incident sea waves, 2, *J. Geophys. Res.* **97**(33): 6790–6801.
- Melville, W. K. (1983). Wave modulation and breakdown, *J. Fluid Mech.* **128**: 489–506.
- Nelson, R. C., P. D. Treloar and N. V. Lawson (1988). The dependency of inshore long waves on the characteristics of offshore short waves, *Coast. Eng.* **12**: 213–231.
- Oltman-Shay, J., P. A. Howd and W. A. Birkemeier (1989). Shear instabilities of the mean longshore current, 2, Field observations, *J. Geophys. Res.* **94**: 18, 031-18, 042.
- Shrira, V. I., V. V. Voronovich and N. G. Kozhelupova (1997). Explosive instability of vorticity waves, *J. Phys. Oceanogr.* **27**: 542–554.

